

## 7 Tesla Cardiac Imaging with a Phonocardiogram Trigger Device

S. Maderwald<sup>1</sup>, S. Orzada<sup>1,2</sup>, Z. Lin<sup>3</sup>, L. C. Schäfer<sup>1,2</sup>, A. K. Bitz<sup>1,2</sup>, O. Kraff<sup>4</sup>, I. Brote<sup>1,2</sup>, L. Häring<sup>3</sup>, A. Czylik<sup>3</sup>, M. O. Zenge<sup>4</sup>, S. C. Ladd<sup>1,2</sup>, M. E. Ladd<sup>1,2</sup>, and K. Nassenstein<sup>1,2</sup>

<sup>1</sup>Erwin L. Hahn Institute for Magnetic Resonance Imaging, Essen, Germany, <sup>2</sup>Department of Diagnostic and Interventional Radiology and Neuroradiology, University Hospital Essen, Essen, Germany, <sup>3</sup>Department of Communication Systems, University of Duisburg-Essen, Essen, Germany, <sup>4</sup>MR Application Development, Siemens AG, Erlangen, Germany

**Introduction:** Ultra-high-field (7T) in vivo cardiac MRI in humans has been reported [1, 2] to present several challenges that have to be overcome before the potentially beneficial increase in SNR and the enhanced soft tissue contrasts at 7 Tesla can be used. To exploit the full potential of cardiac MRI, a number of artifacts and imaging constraints related to 7T have been partly addressed in previous work. New cardiac coil designs [3] and RF shimming approaches (based on simulated or measured  $B_1$  maps [4]) in conjunction with a SAR supervision system [5] enable safe imaging of the heart free of  $B_1$ -related artifacts. One major issue is nevertheless the generation of reliable heart trigger signals. Frauenrath et al. [6] have proposed a MR stethoscope based on a pressure transducer as a gating device free of interference with the high magnetic field. In this study, we used an optoacoustic microphone for direct conversion of the acoustic signal at the subject and acquisition of the Phonocardiogram (PCG).

**Materials and Methods:** The CVMR examinations were performed on a 7-Tesla whole-body MRI system (Magnetom 7T, Siemens Healthcare, Erlangen, Germany). A custom-built flexible 2x4-channel transmit/receive body RF coil driven by 8 power amplifiers (LPPA 13080W, Dressler, Germany) was used for RF signal transmission and reception. For RF shimming, the amplitudes were kept constant for all channels, but the phases of coil channels 1 to 8 were 9°, 278°, 0°, 187°, 252°, 216°, 263°, 42°, respectively. Gating was performed with an optoacoustic microphone (Optimic 4135S, Optoacoustics, Israel) containing no conductive parts and a DSP card (DS1104, dSpace, Germany) for signal detection and trigger generation. To test this device in vivo, 8 healthy volunteers (4 male, 4 female) were examined. Additionally, a patient with known chronic myocarditis, pericardial effusion, and mild arrhythmia was scanned. The vendor ECG unit was utilized for comparison purposes. The imaging protocol encompassed cardiac function along standard views (short and long axis, 4-chamber, 2-chamber, LVOT, LVOT<sup>2nd</sup>) (Cine FLASH: TA 0:28 min), flow measurements at the aortic valve (Cine PC FLASH: VENC 80-110 cm/s, TA 0:29 min), and late-enhancement (LE) sequences (Turbo FLASH\_IR: TI 200-400 ms, TA 0:05 min; FLASH3D\_IR: TI 200-400 ms, TA 0:22 min; and PSIR: TI 200-400 ms, TA 0:05 min). Contrast agent was applied only in the patient. The quality of all images was rated by visual assessment of two radiologists based on signal homogeneity,  $B_0$  and  $B_1$  shim performance, and myocardium-to-blood contrast. Flow measurement results were compared to literature values.

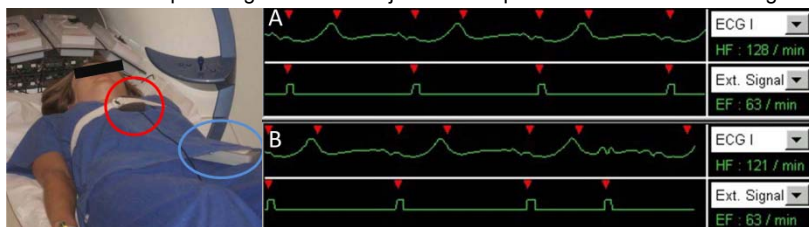


Fig. 1: The PCG microphone is placed on top of the clothes (red circle); the ECG transmitter unit was operated in parallel (blue circle).

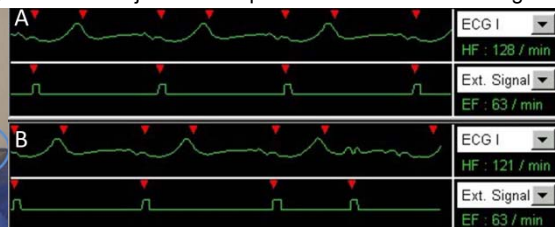


Fig. 2: ECG (top) and external signal (PCG, bottom) A) during normal frequency sinus rhythm and B) during arrhythmic sinus rhythm. Note: The ECG is corrupted by artifacts due to magnetohydrodynamic effects and the electromagnetic fields at 7T, leading to false triggers.

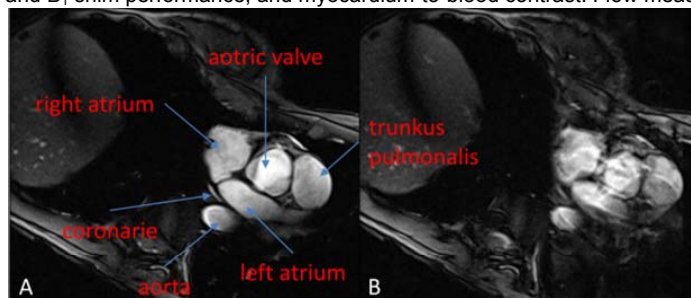


Fig. 3: Comparison between short-axis cine FLASH images gated with A) homebuilt PCG and B) the vendor's ECG. The ECG image reveals severe motion artifacts due to false triggering.

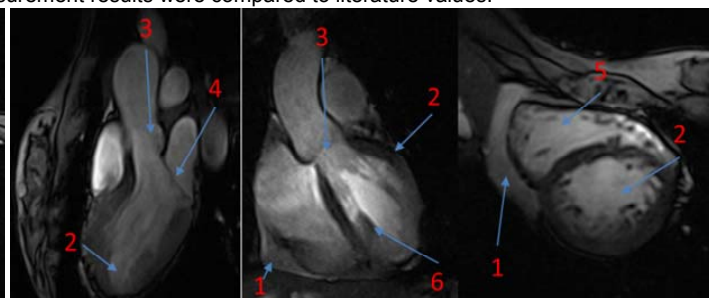


Fig. 4: LVOT, LVOT<sup>2nd</sup>, and short-axis cine FLASH images in the patient. The pericardial effusion is clearly visible (1). (2) Left ventricle, (3) aortic valve, (4) mitral valve, (5) right ventricle, and (6) papillary muscles.

**Results and Discussion:** All subjects tolerated the examination well and could be successfully examined. The placement of the ECG electrodes was adapted as best as possible to 7T issues. The optoacoustic microphone was placed on top of the subject clothing parasternally (Fig. 1). Both outside the 7T magnetic field and at the entry of the scanner bore, the trigger points of the PCG corresponded completely with the ECG and both devices concurrently detected mild arrhythmia in the patient. The standard deviation of the latency between the ECG's R-wave and the PCG's trigger signal outside of the scanner was 4.1 ms for a low-pass filter approach. Please note, the worst-case systematic bias due to the different sampling rates of the vendor ECG (400 Hz) and PCG (200 Hz using the scanner external trigger input) is 2.5 ms. Inside the scanner bore where the ECG waveform was affected by the magnetic field, only the PCG device could be reliably used for gating (Fig. 2 and Fig. 3). The chosen RF shim provided qualitatively good  $B_1$  homogeneity over the heart volume. The Cine FLASH sequence provided good image quality with good signal homogeneity over almost the entire cardiac volume (Fig. 4). Velocity and flow reconstruction of the phase images obtained with the Cine PC FLASH sequence revealed typical results for healthy volunteers for both forward and reverse flow volume and peak velocity. After the injection of double-dose contrast agent (Gadovist 10 ml), the LE sequences (TurboFLASH\_IR, FLASH3D\_IR, PSIR, Fig. 5) revealed the typical time response of the myocardium.

**Conclusion:** The optoacoustic PCG device used in this study enabled reliable cardiac triggering at 7T in volunteers and also in a patient with a mild arrhythmia. The PCG can be placed on top of the clothes, making it very easy to use. A trial should follow to prove its robustness in routine clinical work with patients presenting with different pathologies. Due to the design of the microphone, no safety issues are expected. The acoustic signal is converted immediately to an optical signal, which is conducted via glass fiber out of the scanner. No interaction between the PCG device and the static magnetic field ( $B_0$ ), gradient field, or RF field ( $B_1$ ) was detectable. The ease of use and reliability may make such a device attractive even at lower field strengths.

**References:** [1] Snyder et al., MRM 61:517-524 (2009); [2] Maderwald et al. Proc. ISMRM (2009) (Abstract 821); [3] Maderwald et al. Proc. ISMRM (2010) (Abstract 1300) [4] Bitz et al., Proc. ISMRM (2010) (Abstract 4720); [5] Brote et al., Proc. ISMRM (2009) (Abstract 4788); [6] Frauenrath et al. Invest Radiol 2009; 44: 539-547.

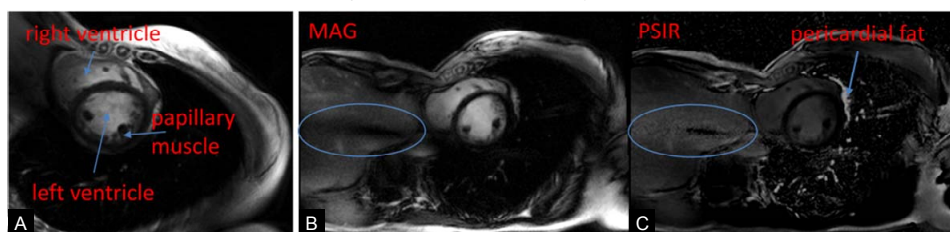


Fig. 5: IR short-axis images. Correct inversion time is indicated by dark myocardium, no enhancement due to contrast media is seen. A) FLASH3D\_IR, B) magnitude image with T1 = 300 ms, normal  $B_1$  inhomogeneity appearance (blue circle) outside ROI, C) PSIR:  $B_1$  inhomogeneity (blue circle) appears as magnified noise.